Ductility of Prestressed and Partially Prestressed Concrete Beam Sections

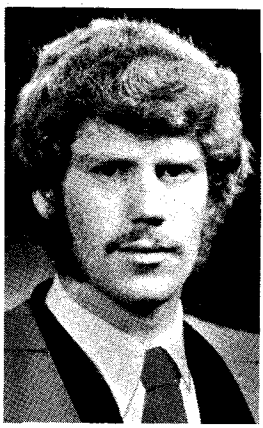

Kevin J. Thompson
Senior Engineer
Ministry of Works and Development
Invercargill, New Zealand

Robert Park
Professor and Head
Department of Civil Engineering
University of Canterbury
Christchurch, New Zealand

Dynamic analyses of structures responding elastically to ground motions recorded during severe earthquakes have shown that the theoretical response inertia loads are generally significantly greater than the static design lateral loads recommended by codes. Hence, structures designed for the lateral earthquake loads recommended by codes can only survive severe earthquakes if they have sufficient ductility to absorb and dissipate seismic energy by inelastic deformations.[1-8]

Prestressed concrete has been widely used for structures carrying gravity loads but has not had the same acceptance for use in structural systems which resist seismic loading. Part of this caution in the use of prestressed concrete for earthquake resistant structures has been due to the paucity of experimental and theoretical studies of prestressed concrete structures subjected to seismic type loading. A survey of the research which has been conducted on the seismic resistance of prestressed concrete was published in 1970.[9] Parme[10] and Hawkins[11] have published more recent reviews of the state of the art of seismic resistance of prestressed and precast concrete.

There has been a lack of detailed building code provisions in the United States for the seismic design of prestressed and precast concrete. For example, the ACI Code,[1] the SEAOC recommendations,[2] the Uniform Building Code,[3] and the tentative provisions of the ATC[4] all contain special provisions for the seismic design of cast-in-place reinforced concrete structures, but do not have

corresponding special provisions for prestressed or precast concrete structures.

According to those codes[2,3,4] precast reinforced concrete frames must comply with all code provisions pertaining to cast-in-place reinforced concrete frames. Englekirk,[12] using an example building developed by Freeman,[13] has recently demonstrated the difficulty of applying the UBC provisions,[3] which were developed for cast-in-place reinforced concrete structures, to ductile precast concrete frames.

American codes discourage the use of prestressed concrete for primary seismic resisting members. For example, the SEAOC recommendations[2] include in its commentary the following statement: "The use of prestressing to develop ductile moment capacity will require testing and is a subject for further study." It is apparent that a similar view is held by other American code committees. The lack of seismic design provisions for ductile prestressed concrete frames is preventing designers from making a proper evaluation of the use of prestressed concrete as an alternative to reinforced concrete.

More progress in the development of seismic provisions for ductile prestressed concrete frames has been made elsewhere. For example, the Commission on Seismic Structures of the FIP[7] has developed such recommendations. Also, the Standards Association of New Zealand[5,6] has recently drafted seismic design recommendations for prestressed concrete based on the significant additional theoretical and experimental information which has become available from recent studies. A summary of that New Zealand work is given in Reference 14.

Prior to developing the main topic of this paper, it is necessary to review the concept of ductility and discuss its design implications.

Synopsis

The results of moment-curvature analyses for a range of prestressed and partially prestressed concrete beam sections are presented. Several models for the stress-strain behavior of the cover concrete are used. The core concrete is modelled using a stress-strain curve which takes into account the influence of confinement.

Derived moment-curvature relations are compared with experimentally measured relations and good agreement is found.

An analytical study is conducted to examine the effect of longitudinal prestressing steel content and distribution, longitudinal non-prestressed steel content and distribution, transverse steel content, and concrete cover thickness on the moment-curvature characteristics of rectangular beam sections, with particular emphasis on the behavior in the post-elastic range.

Conclusions are reached with regard to the effect of the above variables on section ductility.

Design recommendations are made for the detailing of prestressed and partially prestressed concrete beams for ductility for seismic loading.

Design Criteria for Ductility Demand

A ductile structure is one which is capable of large inelastic deformations at near maximum load carrying capacity without brittle failure. Typical ductile load-displacement relations are shown in Fig. 1. The elasto-plastic relation is shown as a dashed line. The relation typical of prestressed concrete is shown as a full curved line.

Nonlinear dynamic analyses of code-designed structures responding to typical severe earthquake motions have given an indication of the order of post-elastic deformations, and hence the "ductility" factor, required. However, the number of variables is so great that no more than qualitative statements can be made at present.

Confusion has existed in the minds of some designers regarding the definition of "ductility factor," since it can be expressed in terms of displacements, rotations or curvatures.

The displacement ductility factor,

$\mu = \Delta_u/\Delta_y$, where:

Δ_u = maximum lateral (horizontal) deflection of the structure and

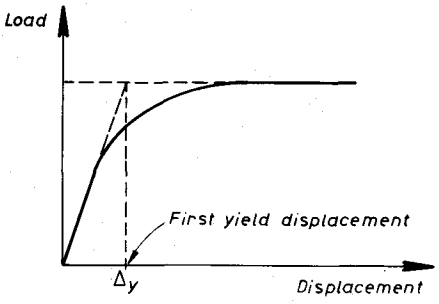

Fig. 1. Load-displacement relation and possible definition of "first yield" displacement. Prestressed concrete is represented by full curved line and elasto-plastic behavior by dashed line.

Δ_y = lateral deflection of the structure at first yield,

is the value commonly determined in nonlinear dynamic analyses.

Some dynamic analyses of frames have used the rotational ductility factor of members, defined at θ_u/θ_y, where:

θ_u = maximum plastic hinge rotation of end of member and

θ_y = rotation at end of member at first yield

The fundamental information needed by the designer concerns the required member section behavior at the plastic hinge expressed by the curvature ductility factor ϕ_u/ϕ_y, where:

ϕ_u = maximum curvature at the section and

ϕ_y = curvature at the section at first yield

Thus, the required ϕ_u/ϕ_y value is a far more meaningful index for ductility demand than the other possibilities. It needs to be recognized that there can be a significant difference between the magnitudes of the displacement, rotational and curvature ductility factors. This is because once plastic hinging has commenced in a structure the deformations concentrate at the plastic hinge positions and further displacement occurs mainly by rotation of the plastic hinges. Thus, the required ϕ_u/ϕ_y ratio will be greater than the Δ_u/Δ_y ratio.[8]

When calculating ductility factors, the definition of first yield deformation (displacement, rotation or curvature) often causes difficulty when the load or moment-deformation curve is not elasto-plastic. This will occur for example due to the stress-strain curve of prestressing steel not having a well defined yield plateau, or to non-prestressed steel bars at different depths in the section yielding at different load levels, or to plastic hinges not

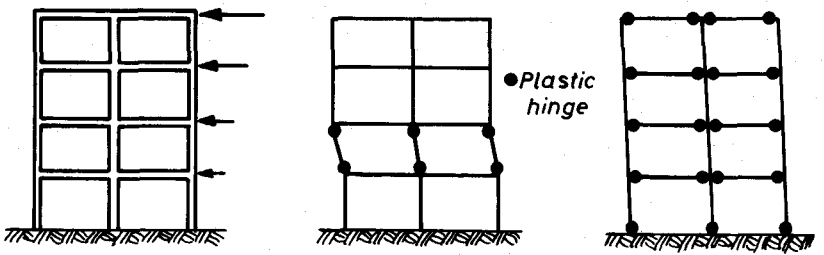

Fig. 2. Building frame under seismic loading and possible mechanisms due to formation of plastic hinges.

forming simultaneously in all members.

In New Zealand[5] the "first yield" displacement is taken as the displacement calculated for the structure assuming elastic behavior up to the strength of the structure in the first load application to yield, as illustrated in Fig. 1. A similar definition can be adopted for first yield rotation and curvature. Such a definition for first yield allows comparison of the effect of different loop shapes, with the same initial stiffness and strength, on the ductility demand.

It is apparent that the sequence of plastic hinge development in structures will influence the curvature ductility demand. Nonlinear dynamic analyses have indicated that ductility demand concentrates in the weak parts of structures and that the curvature ductility demand there may be several times greater than for well proportioned structures. This can also be illustrated by examination of static collapse mechanisms. Fig. 2 shows a frame used for seismic resistance. Possible mechanisms which could form due to development of plastic hinges are also shown in the figure. If plastic hinging commences in the columns of a frame before the beams, a column sidesway mechanism can form. In the worst case the plastic hinges may form in the columns of only one story, since the columns of the other stories are stronger. Such a mechanism can make very large curvature ductility demands on the plastic hinges of the critical story[8] particularly for tall buildings.

On the other hand, if plastic hinging commences in the beams before in the columns a beam sidesway mechanism, as illustrated in Fig. 2, will develop[8] which makes more moderate demands on the curvature ductility required at the plastic hinges in the beams and at the column bases. Therefore, a beam sidesway mechanism is the preferred mode of inelastic deformation, particularly since the straightening and repair of columns is difficult. Hence, for frames, a strong column-weak beam approach is advocated to ensure beam hinging. In the actual dynamic situation higher modes of vibration influence the moment pattern and it has been found[8] that plastic hinges in the beams move up the frame in waves involving a few stories at a time. Thus, the mechanisms shown in Fig. 2 are idealized since they involve behavior under code type static loading. Nevertheless, considerations as in Fig. 2 give the designer a reasonable feel for the situation.

Typical values for the displacement ductility factor μ required of code de-

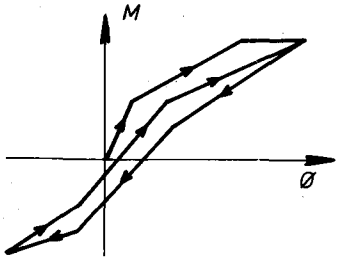

(a) Prestressed Concrete System

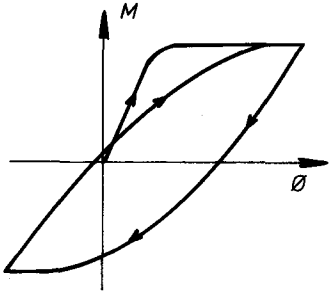

(b) Reinforced Concrete System

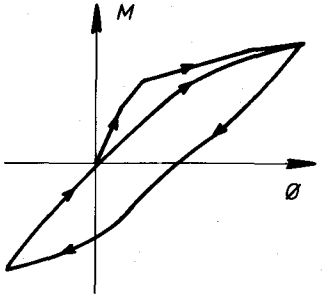

(c) Partially Prestressed Concrete System

Fig. 3. Idealized moment-curvature hysteresis loops for structural concrete systems.

signed ductile frames in order to survive very severe earthquakes are 3 to 5. The tentative provisions of the ATC[4] for ductile frames are based on a value for μ of about 7. The ϕ_u/ϕ_y values required of the plastic hinge sections in a strong column-weak beam design of a framed structure will depend on the geometry of the members. However, it would seem that ϕ_u/ϕ_y of at least 3μ should be available in the plastic hinge regions. Codes do not generally require designers to calculate the actual ductility required at the plastic hinges and then to match that demand. Instead, for reinforced concrete frames the seismic design provisions of codes are intended to ensure that the plastic hinge region will be adequately ductile.

The suspicions that exist concerning prestressed concrete in seismic design are generally a concern whether the energy dissipation at the plastic hinge sections is adequate, and whether such sections can achieve the required ductility. The first issue arises because for prestressed concrete members the initial elastic tensile strain in the tendons due to prestress causes a large deflection recovery, even after large deflections. Hence, the energy dissipation (area within the loop) of prestressed concrete members will be lower than that of reinforced concrete members of similar strength.

Figs. 3(a) and (b) show compared idealized moment-curvature hysteresis loops for cyclically loaded prestressed and reinforced concrete members. Nonlinear dynamic analyses of single degree of freedom systems responding to very severe earthquakes have shown that the maximum displacement of a prestressed concrete system is on average 1.3 times that of a reinforced concrete system with the same code design strength, viscous damping ratio and initial stiffness.[14] However, this effect of lower hysteretic damping should not be an obstacle in design since the ductility required at the sections can be provided in suitably detailed prestressed members.

Note that the moment-curvature loops of prestressed concrete members can be "fattened," and hence the displacement response reduced, if

non-prestressed steel is added to the member to provide the energy dissipation. The presence of longitudinal non-prestressed reinforcing steel also improves the ductility by acting as compression reinforcement. Fig. 3(c) shows a typical moment-curvature loop for partially prestressed concrete.

Scope of Paper

A measure of the ductility of a section can be obtained from the moment-curvature relation plotted to high curvatures. Moment-curvature relations can be derived analytically using idealized models for the stress-strain behavior of the concrete and steel.

In this paper an analytical study is presented which examines the effect of the percentage of longitudinal prestressing steel and its distribution, the percentage of longitudinal non-prestressed steel content and its distribution, the transverse steel content, and the concrete cover thickness, on the curvature ductility of rectangular beam sections.

The aim of the study is to make recommendations for seismic design concerning the distribution of longitudinal and transverse steel within the sections of potential plastic hinge regions in beams of prestressed and partially prestressed concrete frames.

The results summarized in this paper are reported in more detail in Reference 15.

Theoretical Moment-Curvature Analysis

An analysis procedure was developed[15] to determine the moment-curvature relations for prestressed, partially prestressed and reinforced concrete rectangular sections with monotonically applied bending, which allows an assessment of the available ductility. The analysis ensures compatibility of strains and equilibrium of forces and is based on idealizations for the stress-strain behavior of concrete and steel.

Stress-Strain Model for Concrete

The stress-strain relation for confined concrete used is that derived by Kent and Park[16] which covers the full strain range, allowing for the effect of concrete strength and confinement by rectangular hoops on the slope of the "falling branch region." The relation is conservative in that it ignores any enhancement in the maximum concrete strength due to confinement by rectangular hoops. For confinement by typical quantities of closely spaced stirrup ties in the plastic hinge zones of beams the concrete strength may be 10 percent greater than assumed. However, a 10 percent increase in the concrete strength will make little difference to the computed flexural strength of beams. Tests conducted by the Portland Cement Association[17] concluded that the relation gave a simple and reasonable approximation for the stress-strain curve for concrete confined by rectangular hoops.

The stress-strain relation for concrete is illustrated in Fig. 4(a). Expressions for the three compressive regions are as follows:

Region AB: $\epsilon_c \leq \epsilon_o$

$$f_c = f'_c \left[\frac{2\epsilon_c}{\epsilon_{co}} - \left(\frac{\epsilon_c}{\epsilon_{co}} \right)^2 \right] \qquad (1)$$

in which

f_c = concrete stress
f'_c = concrete cylinder strength
ϵ_c = concrete strain, and
ϵ_{co} = 0.002 is the strain in concrete at maximum stress f'_c

Region BC: $\epsilon_{co} < \epsilon_c \leq \epsilon_{20c}$

$$f_c = f'_c \left[1 - Z(\epsilon_c - \epsilon_{co}) \right] \qquad (2)$$

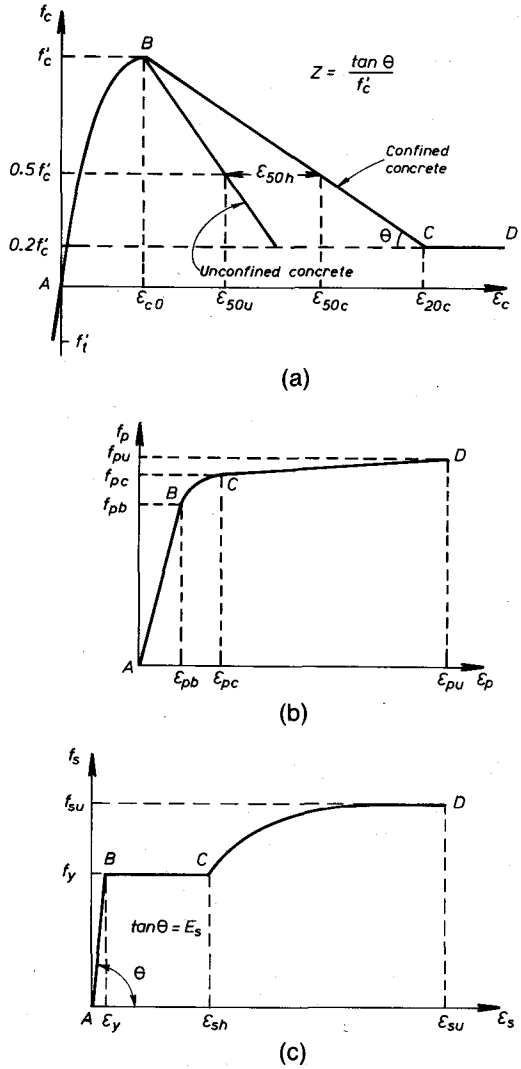

Fig. 4. Assumed stress-strain relations for concrete (top), prestressing steel (middle), and non-prestressed steel (bottom).

in which ϵ_{20c} is the strain at $0.2f'_c$ on the falling branch of the stress-strain curve, and Z defines the slope of the falling branch as follows:

$$Z = \frac{0.5}{\epsilon_{50c} - \epsilon_{co}} \qquad (3)$$

where

$$\epsilon_{50c} = \epsilon_{50u} + \epsilon_{50h}$$

$$= \left[\frac{3 + 0.002f'_c}{f'_c - 1000}\right] + \frac{3}{4}\rho''\sqrt{\frac{b''}{s}} \qquad (4)$$

in which

ρ'' = ratio of volume of hoops to volume of concrete core
b'' = width of concrete core
s = hoop spacing

Note that f'_c is in psi (1 psi = 0.00689 MPa).

The derivation of the empirical Eq. (4) is given in Reference 16.

Region CD: $\epsilon_{20c} < \epsilon_c$

$$f_c = 0.2f'_c \qquad (5)$$

The maximum tensile strength of the concrete (modulus of rupture) is assumed to be given by the expression:

$$f'_t = 7.5\sqrt{f'_c} \qquad (6)$$

in which f'_t and f'_c are in psi.

The stress-strain relation in tension is assumed to follow the slope of the parabola of Region AB of Fig. 4(a) at the origin.

Stress-Strain Model for Prestressing Steel

The stress-strain relation for the prestressing steel in tension used is of the form derived by Blakeley and Park[18] and illustrated in Fig. 4(b). The relation comprises three regions which are defined by the following equations:

Region AB: $\epsilon_p \leq \epsilon_{pb}$

$$f_p = E_p\epsilon_p \qquad (7)$$

in which

ϵ_p = steel strain
ϵ_{pb} = steel strain at Point B (the limit of proportionality)
f_p = steel stress, and
E_p = modulus of elasticity of steel

Region BC: $\epsilon_{pb} < \epsilon_p \leq \epsilon_{pc}$

$$f_p = \frac{f_{pc}\epsilon_{pc} - f_{pb}\epsilon_{pb}}{\epsilon_{pc} - \epsilon_{pb}} + \frac{\epsilon_{pb}\epsilon_{pc}(f_{pb} - f_{pc})}{\epsilon_p(\epsilon_{pc} - \epsilon_{pb})} \quad (8)$$

in which

ϵ_{pc} = steel strain at Point C
f_{pb} = steel stress at Point B
f_{pc} = steel stress at Point C

Region CD: $\epsilon_{pc} < \epsilon_p \leq \epsilon_{pu}$

$$f_p = f_{pc} + \left[\frac{\epsilon_p - \epsilon_{pc}}{\epsilon_{pu} - \epsilon_{pc}}\right](f_{pu} - f_{pc}) \quad (9)$$

in which

ϵ_{pu} = ultimate steel strain
f_{pu} = ultimate steel stress

Numerical values for the stresses and strains at Points B, C, and D need to be obtained from experimentally measured stress-strain curves.

Stress-Strain Model for Non-prestressed Steel

The stress-strain relation for non-prestressed reinforcing steel used is of the form adopted by Park and Paulay[8] and illustrated in Fig. 4(c). The relation is assumed to be identical in tension and compression and comprises three regions which are defined by the following equations:

Region AB: $\epsilon_s \leq \epsilon_y$

$$f_s = E_s\epsilon_s \quad (10)$$

in which

ϵ_s = steel strain
ϵ_y = steel strain at first yield
f_s = steel stress
E_s = modulus of elasticity of steel

Region BC: $\epsilon_y < \epsilon_s \leq \epsilon_{sh}$

$$f_s = f_y \quad (11)$$

in which

ϵ_{sh} = steel strain at commencement of strain hardening, and
f_{sy} = steel stress at yield

Region CD: $\epsilon_{sh} < \epsilon_s \leq \epsilon_{su}$

$$f_s = f_y\left[\frac{Q(\epsilon_s - \epsilon_{sh}) + 2}{60(\epsilon_s - \epsilon_{sh}) + 2} + \frac{(\epsilon_s - \epsilon_{sh})(60 - Q)}{2(30q + 1)^2}\right] \quad (12)$$

where

$$Q = \frac{\frac{f_{su}}{f_y}(30q + 1)^2 - 60q - 1}{15q^2} \quad (13)$$

and

$$q = \epsilon_{su} - \epsilon_{sh} \quad (14)$$

in which

ϵ_{su} = ultimate steel strain, and
f_{su} = ultimate steel stress

Numerical values for stresses and strains at Points B, C, and D need to be obtained from experimentally measured stress-strain curves.

Basic Assumptions

The following assumptions are made for the analysis of the moment-curvature characteristics of prestressed, partially prestressed, and reinforced concrete sections with bonded steel:

1. Plane sections before flexure remain plane after flexure.
2. The bond at the interface of concrete and steel is such that no slip occurs.
3. No time-dependent effects, such as creep, occur during the course of loading.
4. The stress-strain relations for prestressing steel and non-prestressed steel are as given by Eqs. (7) to (14) and as shown in Fig. 4(b) and (c).
5. The stress-strain relation for confined concrete, defined as that concrete within the outside of the perimeter of the hoops, is given by Eqs. (1) to (6) and as shown in Fig. 4(a).

6. The stress-strain relation for the cover concrete, defined as that concrete outside the perimeter of the hoops, is given by one of the following four models:

Model 1—The cover concrete follows the same stress-strain relation as the confined concrete core at all strain levels.

Model 2—The cover concrete follows the same stress-strain relation as the confined concrete core up to a strain of 0.004, at which the cover concrete is assumed to spall and make no further contribution at higher strains.

Model 3—The cover concrete follows the same stress-strain relation as the confined concrete up to a strain of 0.002, and then follows the stress-strain relation for unconfined concrete.

Model 4—The cover concrete follows the same stress-strain relation as the confined concrete up to a strain of 0.002, and then follows the stress-strain relation for confined concrete with a Z value of twice that of the concrete core.

The accuracy of the various models proposed for the cover concrete will be checked by comparison of analytical results with measured test results. Models 1 and 2 represent extremes of behavior and Models 3 and 4 are expected to give more accurate idealizations of the behavior of the cover concrete.

Methods of Analysis

A computer program was developed[15] to compute the moment-curvature relations for rectangular concrete sections containing up to ten bonded prestressing tendon positions and up to ten non-prestressed steel positions anywhere within the section. The moment-curvature relation was found through two loading stages: first, where the neutral axis lies outside the section; and, second, where the neutral axis lies within the section.

An iterative procedure, which satisfies strain compatibility and equilibrium of forces, was used to trace the moment-curvature relation. In the first loading stage a range of moments and their corresponding curvatures were found from a range of neutral axis positions; in the second loading stage a range of moments and their corresponding curvatures were found for a range of extreme fiber concrete compression strains.

At all stages the stress in each prestressing tendon is that corresponding to a total steel strain which is the sum of the steel strain due to prestress when the adjacent concrete strain is zero plus the concrete strain which exists at the level of the steel. The analytical procedure for moment-curvature analyses of sections is well known. Further details may be seen in References 8, 15, 16 and 18.

Comparison of Experimental and Analytical Results

In order to assess the accuracy of the analytical method for the determination of moment-curvature relations, experimental moment-curvature relations measured for a range of prestressed and partially prestressed concrete beams[15,19] were compared with analytical moment-curvature relations derived for the sections.

Experimental Results

The experimental moment-curvature relations were measured in the plastic hinge regions of the beams of the beam-column assembly shown in Fig. 5. The beams and the column were cast in place and represented the part of a continuous frame between the midspan of beams and the mid-height of columns. The columns were

loaded axially as shown and by vertical shears in opposite directions at the ends of the beams.

Horizontal reactive loads were induced at the column ends, and the ends of the column were held in the same vertical line. By reversing the direction of the beam end loads, and hence the direction of the horizontal reactive loads at the column ends, the effects of earthquake loading were simulated. The columns were stronger than the beams and hence plastic hinging occurred in the beams near the column faces rather than in the columns.

The plastic hinge rotation in the beams was measured by dial gages attached to steel frameworks which in turn were attached to pins in the concrete. The curvature plotted was the mean obtained from the measured rotation over a 10 in. (254 mm) or 12 in. (305 mm) gage length in the left beam near the column face of the beam-column test unit during the elastic loading runs and the initial run into the post-elastic range.[15,19] The moment corresponding to this mean measured curvature was taken as that at the center of the gage length.

The curvatures along the beams were also measured along smaller gage lengths during the tests and the equivalent plastic hinge length, l_p, was found to be approximately 9 in. (229 mm), which is one-half of the beam overall depth. It should be appreciated that this is the equivalent plastic hinge length l_p for when the plastic curvature distribution is assumed to be at its maximum value over l_p (that is, an assumed rectangular distribution), whereas the actual distribution of plastic curvature is closer to triangular in shape and extends over a length greater than l_p.

In the subsequent cyclic loading runs into the post-elastic range there was a degradation of stiffness due to loss of cover concrete and cracking in

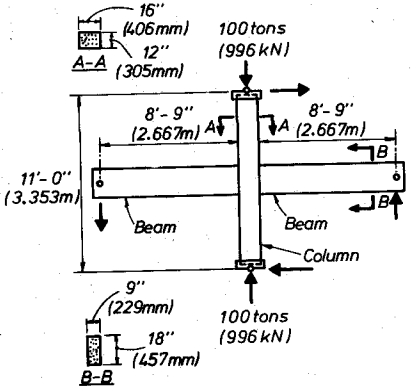

Fig. 5. Dimensions and loading of beam-column test units (References 3 and 6).

the compression zone as a result of loading in the previous direction.[19] However, the flexural strength reached in the beams in the first loading cycle could, in most beams, be reached again in the subsequent load cycles, although at larger deflections. Degradation of flexural strength in subsequent load cycles was only significant in those prestressed beams where non-prestressed compression steel was not present. Idealizations for cyclic load behavior are shown in Fig. 3.

The experimental moment-curvature relations measured in the initial loading run into the post-elastic range for the beams of Units 1, 7, 6, and 3 are shown in Figs. 6, 7, 8, and 9. The main steel and concrete properties of the test beams are shown on the figures. Further details of the test beams are given in References 15 and 19. All beams had approximately the same flexural strength. The beams of Units 1, 7, 6, and 3 had a uniform concrete compressive stress due to prestress at transfer of 1160, 675, 371, and 0 psi (8.0, 4.66, 2.56, and 0 MPa), respectively. The beams of Units 1, 7, 6, and 3 contained non-prestressed longitudinal Grade 40 (f_y = 275 MPa) deformed bars with equal tension and

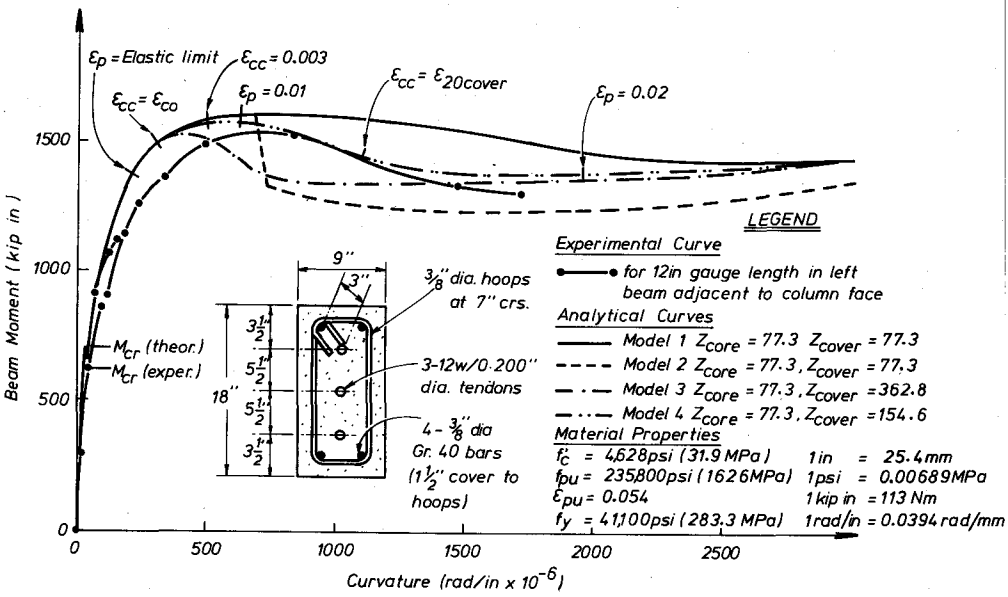

Fig. 6. Experimental and analytical moment-curvature relations for beam of Unit 1.

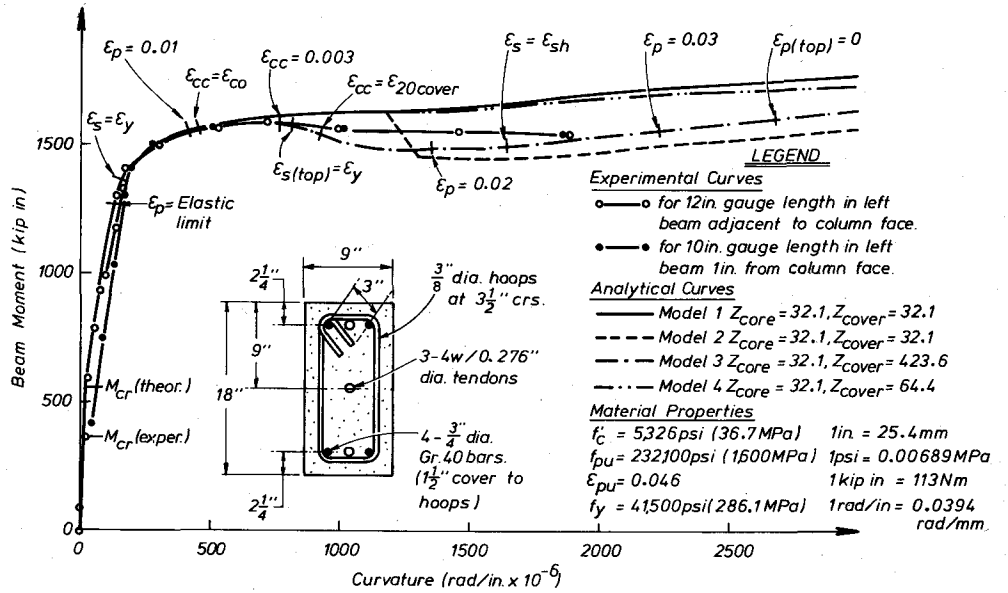

Fig. 7. Experimental and analytical moment-curvature relations for beam of Unit 7.

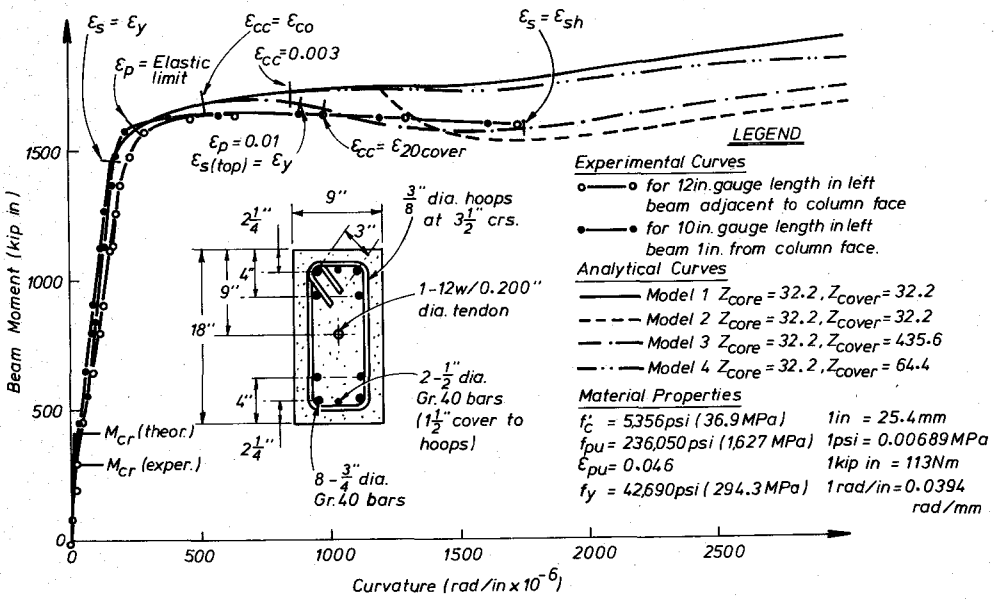

Fig. 8. Experimental and analytical moment-curvature relations for beam of Unit 6.

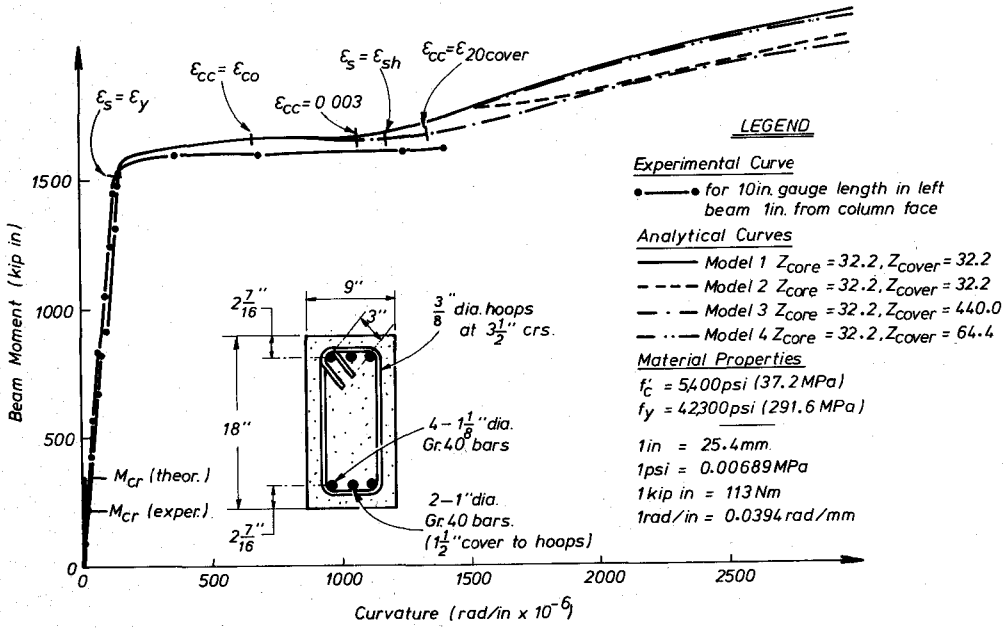

Fig. 9. Experimental and analytical moment-curvature relations for beam of Unit 3.

compression steel ratios of $\rho = \rho' =$ 0.14, 0.57, 1.46, and 1.99 percent, respectively.

Analytical Results

The analytical moment-curvature relations derived for the beams of Units 1, 7, 6, and 3 are shown in Figs. 6, 7, 8, and 9. The analytical relations were derived using the actual properties of each beam and for the four cover concrete models discussed in the assumptions. The strains when various significant stages are reached in the analysis are marked on the analytical curves. The strains shown are:

ϵ_{cc} = strain in concrete in extreme compression fiber

ϵ_p = strain in prestressing steel nearest extreme fiber and

ϵ_s = strain in non-prestressed steel nearest extreme fiber

Comparison of Experimental and Analytical Results

Comparison of the analytical and experimental moment-curvature results shown in Figs. 6, 7, 8, and 9 (and for the other six beams given elsewhere[15]) indicates that the analytical curves fit the experimental results well providing that the appropriate model for the behavior of the cover concrete is selected. When the cover concrete thickness is a small proportion of the section dimensions, the influence of the cover behavior on the moment-curvature relation will be small. In the beam sections shown in Figs. 6, 7, 8, and 9 the ratio of cover concrete thickness to beam width was 1.5/9 = 0.167, which is an upper limit on the ratio likely in beams in practice.

Comparison of the experimental and analytical moment-curvature relations indicates that when a significant amount of non-prestressed compression steel is present (for example, see

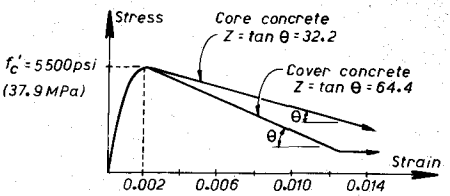

Fig. 10. Assumed stress-strain relation for core concrete and cover concrete (Model 4).

Fig. 9), the influence of the cover concrete behavior on the moment-curvature curve is very small. It has been observed previously[18] that the presence of hoops at small spacing results in a plane of weakness between the cover concrete and the core concrete and tends to precipitate the spalling of the cover concrete at high strains. Conversely, with a large hoop spacing the cover and core concrete will act more monolithically and tend to follow the same stress-strain curve.

Inspection of the experimental and analytical moment-curvature relations compared in the figures shows that for the beam of Unit 1 with a hoop spacing of 0.39 times the beam overall depth, Model 4 ($Z_{cover} = 2Z_{core}$) gave the best fit and Model 3 ($Z_{cover} = Z_{unconfined}$) gave the next best fit. For the beams of the other units with a hoop spacing of 0.19 times the beam overall depth, Model 3 ($Z_{cover} = Z_{unconfined}$) gave the best fit and Model 4 ($Z_{cover} = 2Z_{core}$) and Model 2 ($Z_{cover} = Z_{core}$, but cover concrete ignored at strains greater than 0.004) also gave reasonable fits. In general, it appears that either Model 4 or Model 3 could be used in analysis with good results, that Model 2 is generally conservative, and that Model 1 is generally unconservative.

This analytical approach does not consider deformations due to shear. The maximum shear forces present in the beams of the test units were not high, the maximum nominal shear

stress $V_u/0.8hb$ present in the beams being only $1.78\sqrt{f'_c}$ psi ($0.147\sqrt{f'_c}$ MPa). The diagonal tension cracking was not significant in the beam plastic hinge zones and it was evident that for these beams shear had little effect on the moment-curvature characteristics.

General Analytical Moment-Curvature Study

The effects of longitudinal prestressing steel and non-prestressed steel content and distribution, transverse steel content and cover concrete thickness, on the moment-curvature characteristics of rectangular concrete sections were studied analytically with particular emphasis on the behavior in the post-elastic range at high curvatures.

For all cases studied the ultimate tensile strain of the prestressing steel was taken as 0.035, which was the minimum value obtained from the experimental tests on the prestressing steel associated with the tests reported.[15,19] Also, the strain in the prestressing steel due to prestress alone was taken as 0.0057, which was the strain which gave an initial steel stress equal to 70 percent of the ultimate tensile stress.

The beams are assumed to be confined by rectangular hoops. For those sections in which $Z_{core} = 32.2$ is specified, the confinement can be regarded as being provided by ⅜ in. (9.5 mm) diameter hoops at 3½ in. (89 mm) centers confining a 15 in. (381 mm) deep by 6 in. (152 mm) wide concrete core, and the cover concrete can be regarded as being that 1½ in. (38 mm) thickness of concrete between the hoops and the edges of the 9 in. (228 mm) wide by 18 in. (457 mm) deep section. However, since the curves have been plotted non-dimensionally, they apply generally to other geometrically similar sections with the specified Z values and ratio of cover concrete thickness to beam section dimension.

Fig. 10 shows the idealized stress-strain curves for the concrete when $Z = 32.2$ and $Z = 64.4$, and illustrates the degree of ductility available from confinement corresponding to those Z values.

Effect of Content of Prestressing Steel on Ductility

The effect of prestressing steel content* on the moment-curvature characteristics, and hence the ductility, of sections is of interest. The analytical moment-curvature relations for rectangular beam sections using the dimensionless coordinates ϕh and $M/f'_c bh^2$, and the assumed section parameters are plotted in Figs. 11, 12, and 13. The cover concrete behavior is assumed to be described by cover concrete Model 4 with $Z_{core} = 32.2$ and $Z_{cover} = 64.4$. The abrupt reduction of moment at high curvatures in Figs. 12 and 13 (and in some subsequent figures) occurs when the prestressing steel reaches its ultimate (fracture) strain.

Fig. 11 shows curves for a section eccentrically prestressed by one tendon at a depth of $0.8h$ for a range of prestressing steel contents specified as A_{ps}/bh ratios.

ACI 318-77[1] and the UBC[3] require that for prestressed concrete beams in gravity load design the longitudinal steel used to calculate the flexural strength should satisfy:

$$A_{ps}f_{ps}/bdf'_c \leq 0.3 \qquad (15)$$

where f_{ps} is the prestressing steel stress at maximum moment.

This requirement is intended to ensure that beams designed to resist gravity loading have some ductility.

*The term "prestressing steel content" expresses the ratio A_{ps}/bh.

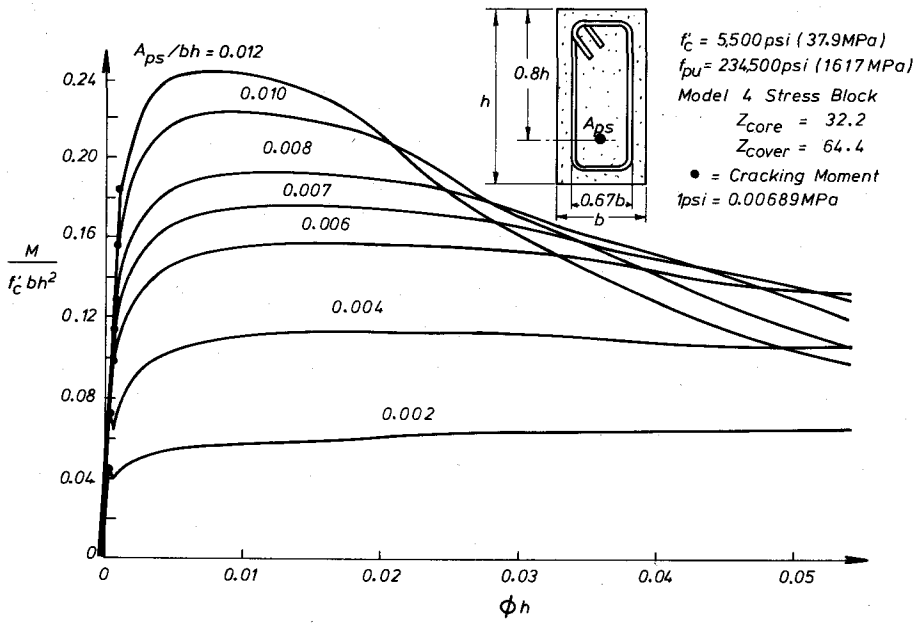

Fig. 11. Effect of content of prestressing steel on analytical moment-curvature relation with one tendon position.

Eq. (15) gives $A_{ps}/bh \leq 0.0069$ when $d = 0.8h$, $f'_c = 5500$ psi (37.9 MPa), $f_{pu} = 234{,}500$ psi (1617 MPa) and f_{ps} is as given by the ACI Code[1] and the UBC[3] for members with bonded prestressing tendons. A moment-curvature curve for $A_{ps}/bh = 0.007$ is plotted in Fig. 11 and it is evident that this code limitation on prestressing steel area for flexural strength calculations results in moderate ductility which is probably satisfactory for gravity loading. However, these codes allow the steel area placed to exceed that specified by Eq. (15), provided that the excess steel area is not included in the flexural strength calculations. It is evident that, if a greater steel area than is specified by Eq. (15) is placed, a brittle flexural failure can actually occur, although at a higher moment, even though the additional steel is ignored in the flexural strength calculations.

For seismic loading, it is desirable for the moment to be maintained near the maximum value over a greater curvature range. Hence, a more severe limitation on the maximum steel area should be used, and this maximum should not be exceeded even if any excess steel area is not included in the flexural strength calculations. Any excess steel area will lower the section ductility and the enhanced flexural strength may result in a shear failure. To ensure reasonable ductility in seismic design, it is suggested that the 0.3 on the right hand side of Eq. (15) be replaced by 0.2. This would give an absolute limiting value of $A_{ps}/bh = 0.0046$ in Fig. 11, which would result in the section having significantly better ductility. Thus, for seismic design, the requirement for plastic hinge regions of beams when the prestressing tendons are concentrated near the extreme tension fiber should be:

$$A_{ps}f_{ps}/bdf'_c \leq 0.2 \qquad (16)$$

Figs. 12 and 13 show the moment-curvature relations for sections con-

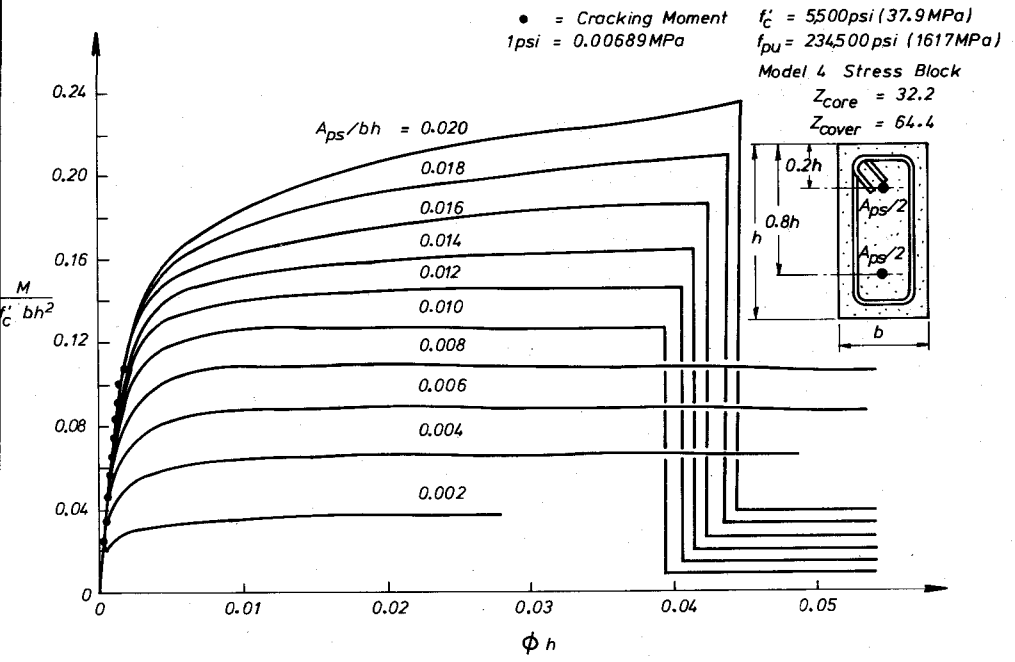

Fig. 12. Effect of content of prestressing steel on analytical moment-curvature relation with two tendon positions.

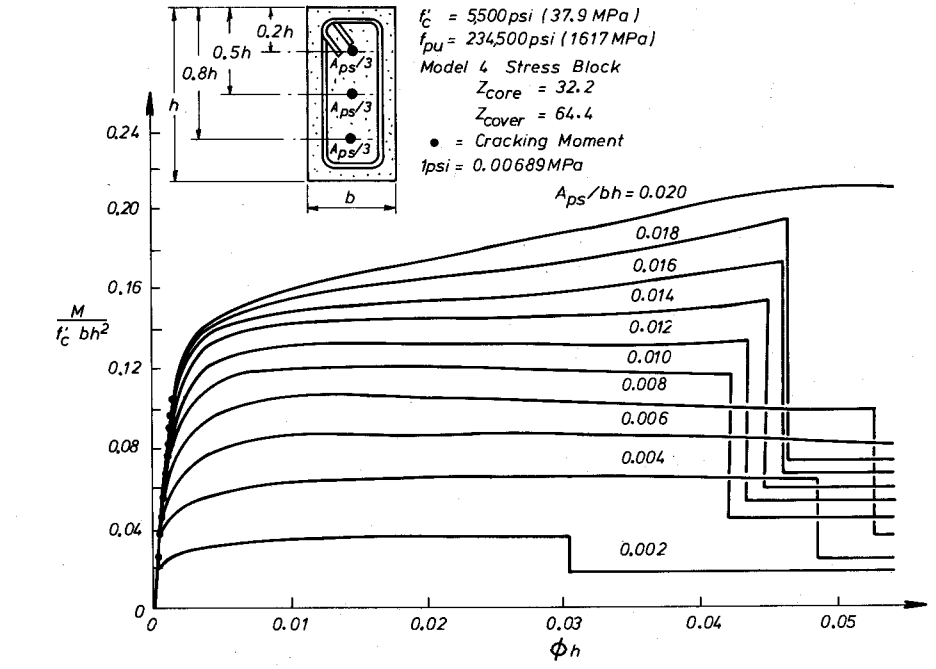

Fig. 13. Effect of content of prestressing steel on analytical moment-curvature relation with three tendon positions.

centrically prestressed with two and three tendons, respectively, for a range of A_{ps}/bh ratios. These two figures show that with prestressing steel present in the concrete compression region, an increase in prestressing steel content does not lead to a reduction in ductility. This is because, provided that the top prestressing steel is restrained from buckling in compression by the surrounding confined concrete and confining steel, the top prestressing steel can act as compression reinforcement at high concrete compression strains, thus maintaining the compression force at a position near the top of the section.

Successive cycles of reversed flexure during seismic loading may cause damage to concrete leading to buckling of tendons. Hence, it does not appear advisable to take advantage of the extremely high ductilities that may be available at very high concrete strains. It would appear reasonable to require that all beam sections are capable of reaching a specified curvature at a given extreme fiber compressive concrete strain.

This criterion means that at the ultimate moment the neutral axis depth should not exceed some limiting value. For example, Eq. (16) suggests that for beams with rectangular sections having prestressing steel concentrated near the extreme tension fiber, the requirement should be $A_{ps}f_{ps} \leq 0.2f'_c bd$. Since $A_{ps}f_{ps}$ is the tendon tensile force this means that the maximum possible compressive force in the concrete at the flexural strength is $0.2f'_c bd$. The compressive force in the concrete is given by $0.85f'_c ab$ at this stage and hence the maximum possible depth of the rectangular concrete compressive stress block is:

$$a = \frac{0.2f'_c bd}{0.85f'_c b}$$

$$= 0.235d$$

But since d is approximately $0.8h$ and a is about $0.75c$ [when $f'_c = 6000$ psi (41.4 MPa)], where c is the neutral axis depth at the flexural strength, then

$$a \leq 0.2h \qquad (17a)$$

$$\text{or } c \leq 0.25h \qquad (17b)$$

For sections with tendons at various positions down the depth of the member, it is difficult to set a limiting value of $A_{ps}f_{ps}/bdf'_c$ because tendons at various levels result in sections with different moment-curvature characteristics from the case when all the tendons are placed near the extreme tension fiber. Rather than stipulating different limiting values for $A_{ps}f_{ps}/bdf'_c$ for various tendon positions in the section, it is more convenient to require $a/h \leq 0.2$ or $c/h \leq 0.25$ for all sections.

This requirement achieves the same end result for all sections since the curvature at ultimate moment will always be at least equal to that of the section with all tendons placed near the extreme tension fiber. Eq. (17) has been adopted by the FIP recommendations[7] and the draft New Zealand Concrete Design Code[6] for seismic design of prestressed and partially prestressed concrete sections.

Effect of Distribution of Prestressing Steel on Ductility

In seismic design the reversals of moment in beams near column faces during earthquake shaking will require the section to have both negative and positive moment strength, and hence tendons will exist near both extreme fibers of the section and near middepth. Thus, the effect of the distribution of the prestressing steel within the section, while maintaining a concentric steel arrangement, is a variable of interest.

Moment-curvature curves were derived for sections with from one to

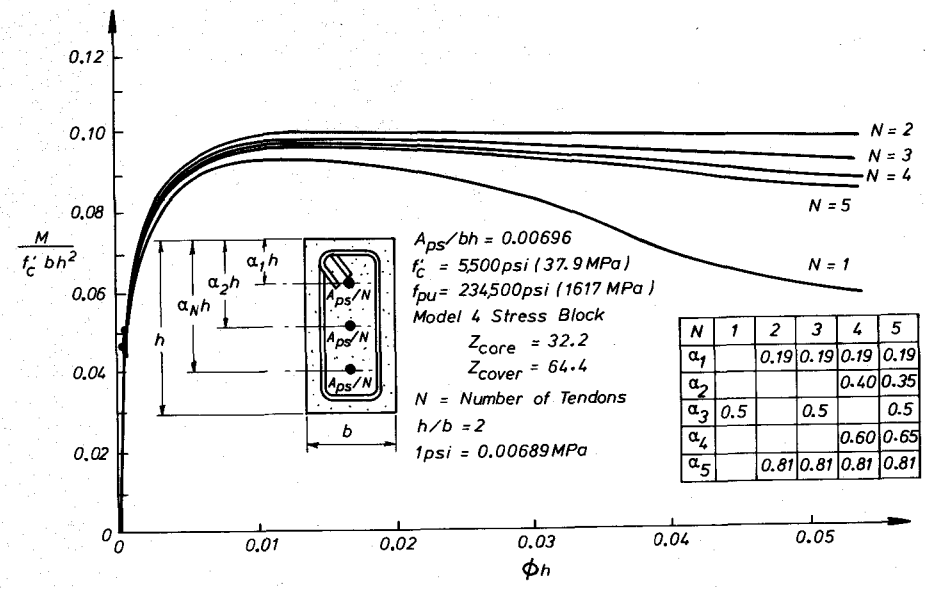

N	1	2	3	4	5
α_1		0.19	0.19	0.19	0.19
α_2				0.40	0.35
α_3	0.5		0.5		0.5
α_4				0.60	0.65
α_5		0.81	0.81	0.81	0.81

Fig. 14. Effect of distribution of prestressing steel on analytical moment-curvature relation.

five tendons symmetrically distributed down the depth. The total steel content is the same for each of the five cases being $A_{ps}/bh = 0.00696$ (which corresponds to that of Unit 1.[15,19]) The stress-strain behavior of the cover concrete is described by Model 4, with $Z_{core} = 32.2$ and $Z_{cover} = 64.6$.

The analytical moment-curvature curves using the dimensionless coordinates ϕh and $M/f'_c bh^2$ are compared in Fig. 14. The moment-curvature curves for $N = 2$ to $N = 5$, where N is the number of tendons, are reasonably similar, and these sections are able to maintain near maximum moment capacity at high curvatures. For the sections with one tendon, $N = 1$, the internal lever arm is smaller and there are no tendons to act as "compression reinforcement." Hence, when $N = 1$ the section is more sensitive to any increase in the neutral axis depth due to deterioration of the compressed concrete, and the moment capacity reduces significantly at high curvatures. Thus, for sections subjected to seismic load reversals it is desirable to have two or more prestressing tendons within the section, with at least one tendon near the top and one near the bottom edges of the section.

Effect of Transverse Reinforcement on Ductility

A significant variable affecting the ductility of prestressed concrete members is the degree of confinement of the concrete in the compression region provided by transverse reinforcement in the form of rectangular steel hoops (also referred to as stirrup ties).

Fig. 15 shows analytical moment-curvature curves using the dimensionless coordinates ϕh and $M/f'_c bh^2$ drawn for sections with three prestressing tendons and various transverse steel contents. The prestressing arrangement is similar to that of the beam of Unit 1.[15,19] The curves are drawn for ⅜ in. (9.5 mm) diameter hoops at spacings varying between $s = 7$ to 1 in. (178 to 25 mm) with 1½

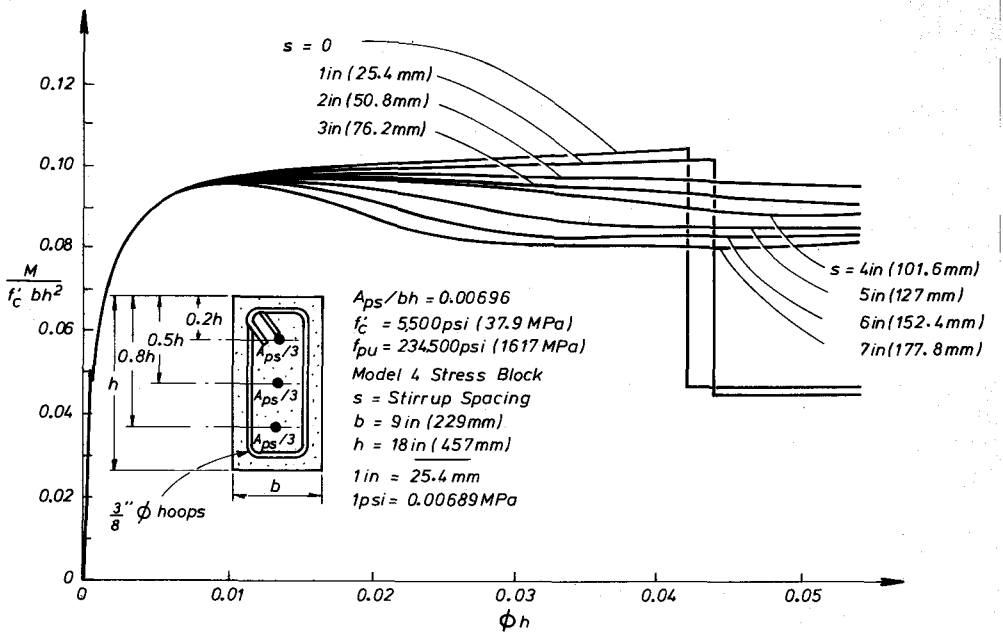

Fig. 15. Effect of hoop spacing on analytical moment-curvature relation.

in. (38.1 mm) cover to the hoops. A similar model for the cover concrete was used for all cases, this being Model 4 ($Z_{cover} = 2Z_{core}$), since it can be applied with reasonable accuracy to beams with both small and large hoop spacings.

Fig. 15 indicates that some advantage is to be gained from extra core confinement. For the particular section being considered, with an overall depth of h = 18 in. (457 mm), a hoop spacing of $d/4$ where $d = 0.8h$ would mean a spacing of 3.6 in. (91 mm) which would lead to reasonable ductility. Unfortunately, the tendency for the cover concrete to spall increases as the hoop spacing decreases and thus the moment capacity of sections with close hoop spacing at high curvatures will not be as great as shown in Fig. 15, since Model 2 would be more applicable to the cover concrete.

Some advantages of close hoop spacing not evident from this study of beams under monotonic loading are the reduction of the crushing of the core concrete between the hoops during cyclic loading, and the confinement of the concrete surrounding the prestressing steel in the compression region thus preventing possible steel buckling.[8,15,19]

Effect of Cover Thickness on Ductility

After a prestressed concrete member has sustained large curvatures the cover concrete partly crushes and disintegrates. After several cycles of reversed loading have been sustained in the inelastic range the cover concrete tends to spall off completely and does not contribute to the moment-curvature behavior. In order to study the effect of the loss of the cover concrete on the moment capacity and ductility of prestressed concrete members, the analytical moment-curvature relations of a prestressed concrete section (with the same size, prestressing steel content and arrangement as Unit 1[15,19]) are plotted in Fig. 16 using the dimensionless coor-

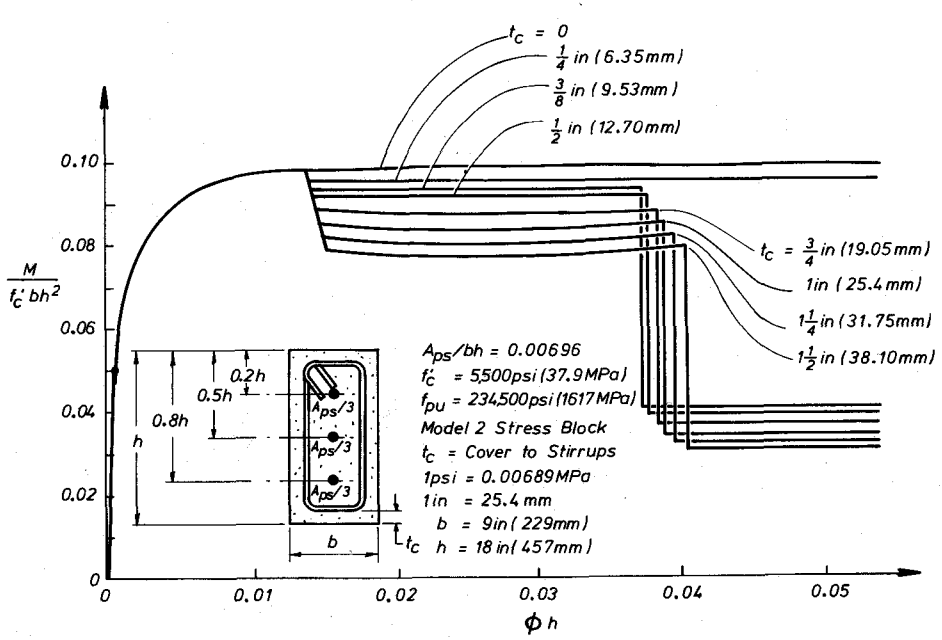

Fig. 16. Effect of cover concrete thickness on analytical moment-curvature relation.

dinates ϕh and $M/f'_c bh^2$ for values of cover concrete thickness t_c from 0 to 1½ in. (38 mm). Model 2 is used to describe the cover concrete behavior; that is, the cover concrete follows the same stress-strain relation as the core concrete until a concrete compressive strain of 0.004 is reached, and then spalls and makes no further contribution.

The curves in Fig. 16 show that the moment capacity of the section of width 9 in. (229 mm) and overall depth of 18 in. (457 mm) and with 1½ in. (38 mm or $0.083h$) cover thickness drops 20 percent when the cover concrete spalls, while the section with ⅜ in. (9.5 mm or $0.021h$) cover thickness shows a reduction of only 3.5 percent in moment capacity subsequent to the spalling of the cover concrete. If the sections with a cover thickness of less than 1½ in. (38 mm) are considered to be scale models, then for larger members with cover thicknesses conforming to ACI 318-77[1] and to the UBC[3] the effect of the loss of cover concrete is not as great as for a smaller member conforming to the same cover requirements.

Effect of Prestressing Steel Content in Partially Prestressed Beams

Fig. 17 shows the analytical moment-curvature relations derived for a partially prestressed concrete section with equal quantities of non-prestressed steel in the top and bottom of the section ($A_s/bh = A'_s/bh = 0.0062$) and for various values of prestressing steel content expressed by the ratios of A_{ps}/bh. This figure shows that an increase in strength is achieved with increasing A_{ps}/bh without a great reduction in ductility.

It can be concluded that provided sufficient non-prestressed compression reinforcement is present, the inclusion of a central prestressing tendon in the section can benefit the behavior of the beam by delaying cracking and increasing the strength without much reduction in ductility, at least up to

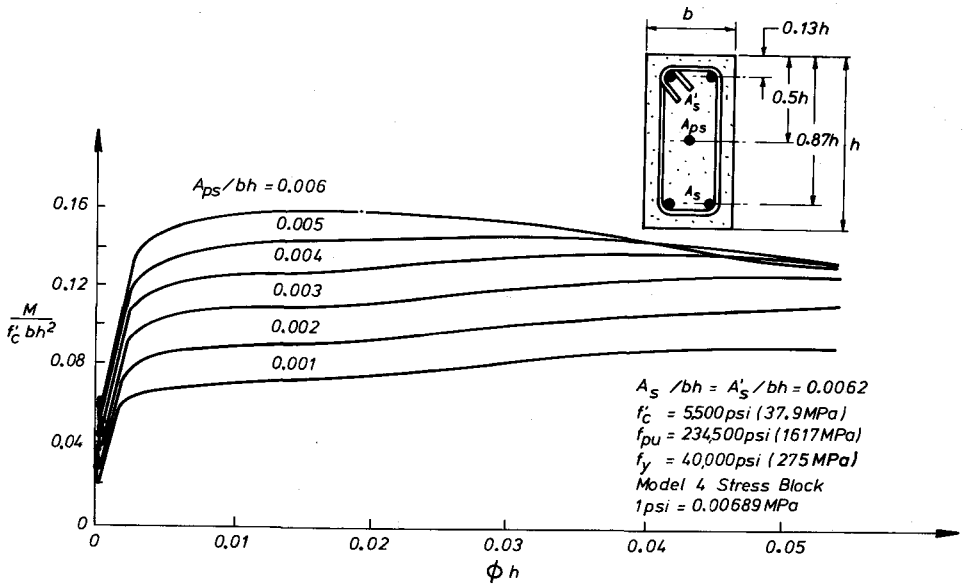

Fig. 17. Effect of prestressing steel content on analytical moment-curvature relation of partially prestressed concrete beam.

the limiting a/h ratio proposed in Eq. (17). Also, tests[15,19] have demonstrated clearly that in seismic design it is desirable to have some non-prestressed longitudinal steel present near the extreme fibers of the section since it leads to an increase in ductility by acting as compression reinforcement and results in an increase in energy dissipation by fattening out the moment-curvature hysteresis loops under cyclic flexure.

Conclusions

The following is a summary of the major conclusions based on the results of the investigation of the moment-curvature behavior, and hence the ductility, of prestressed and partially prestressed concrete beam sections:

1. Comparison of Analytical and Experimental Results for Prestressed and Partially Prestressed Concrete Beams

The analytical moment-curvature relations fitted experimentally measured moment-curvature relations well, providing that the appropriate model for the stress-strain behavior of the cover concrete is chosen. When a significant amount of non-prestressed compression steel is present, or the thickness of cover concrete is small, the influence of concrete cover behavior on the moment-curvature relation *is not* significant. However, a large thickness of concrete cover over the hoops in prestressed concrete beams will normally have a significant influence on the moment-curvature behavior.

In the moment-curvature studies it was found to be unconservative to assume that the concrete cover had the same stress-strain behavior as the confined concrete core, and overly conservative to assume that the concrete cover crushes and is lost at strains greater than 0.004. The best fit with the experimental results was obtained when the concrete cover was assumed to have a stress-strain curve with a falling branch slope of either than of unconfined concrete or that of twice the confined concrete.

2. Prestressed Concrete Beams

(a) Effect of Content of Prestressing Steel on Ductility — The analytical study showed that moderately ductile behavior can be achieved in prestressed concrete sections eccentrically prestressed up to the ACI 318-77 and UBC limitation of:

$$A_{ps}f_{ps}/bdf'_c \leq 0.3$$

but that a more satisfactory limit for prestressing steel content, which ensures more reasonable ductility for seismic design, would be given by:

$$A_{ps}f_{ps}/bdf'_c \leq 0.2$$

In beam sections which are concentrically prestressed with a symmetrical arrangement of tendons, including tendons in both the top and bottom of the section, satisfactory ductility can be achieved almost regardless of the prestressing steel content providing that buckling of the prestressing tendons does not occur. A suitable criterion for seismic design which would ensure ductility regardless of the positions of the tendons in the section would be to require $a \leq 0.2h$ in all cases.

(b) Effect of Distribution of Prestressing Steel on Ductility — When subject to reversed moments, such as in seismic design, prestressed concrete beams need to have both positive and negative moment strength. The analytical study showed that prestressed concrete beam sections which are concentrically prestressed with two or more tendons placed symmetrically in the section, including at least one tendon in the top and one in the bottom of the section, achieve a greater ductility than a section with the same prestressing steel content concentrated only at the middepth of the section. Hence, reversed moment strength is best obtained by placing some tendons near both extreme fibers of the section rather than placing all the tendons at middepth.

(c) Effect of Transverse Reinforcement on Ductility — The analytical study showed that the presence of hoops had a beneficial effect on the ductility of prestressed concrete members because of the confinement of the concrete. Such transverse steel is also necessary to prevent buckling of longitudinal steel and to prevent progressive damage of core concrete when subject to cyclic loading.

(d) Effect of Cover Thickness on Ductility — The analytical study showed that a small concrete cover thickness ensures that a prestressed concrete beam section when subject to large curvatures does not undergo a significant reduction in the moment capacity once the concrete cover spalls. From the viewpoint of ductility, the concrete cover thickness should be made as small as possible.

3. Partially Prestressed Concrete Beams

The analytical study showed that the introduction of a prestressing tendon at the middepth of a concrete section which is doubly reinforced equally top and bottom by non-prestressed steel, increases the cracking and flexural strengths of the section without significant reduction in ductility, at least up to the proposed limit of a/h ratio. The presence of non-prestressed steel in the section is desirable in seismic design since it acts as compression reinforcement, reduces degradation of moment strength during cyclic loading and increases the energy dissipation of the member.

Design Recommendations

Based on the findings of this study, plus the authors' judgment and experience, the following design recommendations are suggested for the

detailing of prestressed and partially prestressed concrete beams for ductility subject to seismic loading:

1. The content of prestressed plus non-prestressed steel should be such that at the flexural strength at potential plastic hinge regions, $a/h \leq 0.2$, where a = depth of rectangular concrete compressive stress block and h = overall depth of section.

2. In potential plastic hinge regions of beams, the spacing of hoops should not exceed $d/4$ or 6 in. (150 mm), where d = effective depth of section but d need not be more than $0.8h$. The distance between the vertical legs of hoops across the section should not exceed 8 in. (200 mm) in each set of hoops.

3. Except as provided in Item 4 below, the prestressing tendons in potential plastic hinge regions of beams should be grouted and should be placed so that at least one tendon is located at not more than 6 in. (150 mm) from the beam top, at least one within the middle third of the beam depth, and at least one at not more than 6 in. (150 mm) from the beam bottom.

4. When partially prestressed beams are designed with non-prestressed steel reinforcement in the extreme fibers of potential plastic hinge regions providing at least 80 percent of the seismic resistance, the prestress may be provided by one or more tendons located within the middle third of the beam depth. In such cases post-tensioned tendons may be ungrouted, provided anchorages are detailed to ensure that anchorage failure, or tendon detensioning, cannot occur under seismic loads.

Acknowledgment

The work described herein formed part of an investigation conducted in the Department of Civil Engineering of the University of Canterbury, New Zealand, by K. J. Thompson during his PhD studies under the supervision of R. Park. The authors are particularly grateful for the financial assistance of the University of Canterbury, University Grants Committee, Ministry of Works and Development, Building Research Association (New Zealand) and the New Zealand Prestressed Concrete Institute.

* * *

Note: A Notation section is given on the page following the references.

Discussion of this paper is invited. Please send your comments to PCI Headquarters by Sept. 1, 1980.

REFERENCES

1. ACI Committee 318, "Building Code Requirements for Reinforced Concrete (ACI 318-77)," American Concrete Institute, Detroit, 1977, 102 pp.
2. *Recommended Lateral Force Requirements and Commentary,* Seismology Committee, Structural Engineers Association of California, San Francisco, 1975, 21pp. plus commentary and appendices.
3. *Uniform Building Code,* International Conference of Building Officials, Whittier, California, 1979.
4. *Tentative Provisions for the Development of Seismic Regulations for Buildings,* Applied Technology Council, US Government Printing Office, Washington, 1978, 505 pp.
5. *Code of Practice for General Structural Design and Design Loadings for Buildings (NZS 4203:1976),* Standards Association of New Zealand, 1976, 80 pp.
6. *Draft Code of Practice for the Design of Concrete Structures (DZ 3101),* Standards Association of New Zealand, 1978.
7. Commission on Seismic Structures, *Recommendations for the Design of Aseismic Prestressed Concrete Structures,* Fédération Internationale de la Précontrainte, London, 1977, 28 pp.
8. Park, R., and Paulay, T., *Reinforced Concrete Structures,* John Wiley & Sons, New York, 769 pp.
9. Blakeley, R. W. G., Park, R., and Shepherd, R., "A Review of the Seismic Resistance of Prestressed Concrete," *Bulletin,* New Zealand Society for Earthquake Engineering, V. 3, No. 1, March, 1970, pp. 3-23.
10. Parme, A. L., "American Practice in Seismic Design," PCI JOURNAL, V. 17, No. 4, July-August 1972, pp. 31-44.
11. Hawkins, N. M., "State-of-the-Art Report on Seismic Resistance of Prestressed and Precast Concrete Structures (Part 1 and 2)," PCI JOURNAL, V. 22, No. 6, November-December 1977, pp. 80-110 and V. 23, No. 1, January-February 1978, pp. 40-58.
12. Englekirk, R. E., "Development of a Precast Concrete Ductile Frame," PCI JOURNAL, V. 24, No. 6, November-December 1979, pp. 46-65.
13. Freeman, S. A., "Seismic Design Criteria for Multistory Precast Prestressed Buildings," PCI JOURNAL, V. 24, No. 3, May-June 1979, pp. 62-88.
14. Park, R., "Design of Prestressed Concrete Structures," *Proceedings,* Workshop on Earthquake Resistant Reinforced Concrete Building Construction, V. III, University of California, Berkeley, July 1977, pp. 1722-1752.
15. Thompson, K. J., "Ductility of Concrete Frames Under Seismic Loading," Doctor of Philosophy Thesis, University of Canterbury, New Zealand, 1975, 341 pp. plus appendices.
16. Kent, D. C., and Park, R., "Flexural Members with Confined Concrete," *Journal of the Structural Division,* ASCE, V. 97, No. ST7, July 1971, pp. 1969-1990.
17. Kaar, P. H., Fiorata, A. E., Carpenter, J. E., and Corley, W. G., "Earthquake Resistant Structural Walls—Concrete Confined by Rectangular Hoops," Research and Development Concrete Construction Laboratories, Portland Cement Association, Skokie, 1976, 30 pp.
18. Blakeley, R. W. G. and Park, R., "Prestressed Concrete Sections With Seismic Loading," *Journal of the Structural Division,* ASCE, V. 99, ST8, August 1973, pp. 1717-1742.
19. Park, R., and Thompson, K. J., "Cyclic Load Tests on Prestressed and Partially Prestressed Concrete Beam-Column Joints," PCI JOURNAL, V. 22, No. 5, September-October 1977, pp. 84-110.

NOTATION

A_{ps} = total prestressing steel area
A_s = total area of non-prestressed tension steel
A'_s = total area of non-prestressed compression steel
a = depth of concrete rectangular compressive stress block at flexural strength
b = width of concrete section
b'' = width of confined core measured to outside of hoops
c = neutral axis depth at flexural strength measured from extreme concrete compression fiber
d = distance from extreme compression fiber to centroid of tension steel but in the case of a prestressed concrete member not less than 0.8 times the overall depth of the member
E_p = modulus of elasticity of prestressing steel
E_s = modulus of elasticity of non-prestressed steel
f_c = concrete stress
f'_c = concrete compressive cylinder strength
f_p = prestressing steel stress
f_{pb} = prestressing steel stress defined in Fig. 4(b)
f_{pc} = prestressing steel stress defined in Fig. 4(b)
f_{ps} = stress in prestressing steel at flexural strength
f_{pu} = ultimate strength of prestressing steel
f_s = stress in non-prestressed steel
f_{su} = ultimate strength of non-prestressed steel
f'_t = tensile strength (modulus of rupture) of concrete
f_y = yield strength of non-prestressed steel
h = overall depth of concrete section
l_p = equivalent plastic hinge length
M = moment
N = number of prestressing steel tendons
s = spacing of transverse reinforcement
t_c = cover concrete thickness
V_u = shear force
Z = slope of falling branch of concrete stress-strain curve defined by Eq. (3)
Z_{core} = value of Z for core concrete
Z_{cover} = value of Z for cover concrete
Δ_u = ultimate displacement
Δ_y = displacement at first yield
ϵ_{20c} = concrete strain at $0.2f'_c$ on falling branch of concrete stress-strain curve
ϵ_{50c} = concrete strain at $0.5f'_c$ on falling branch of concrete stress-strain curve [see Eq. (4)]
ϵ_{50h} = additional strain due to confinement of concrete at $0.5f'_c$ on falling branch of concrete stress-strain curve
ϵ_{50u} = strain at $0.5f'_c$ on falling branch of unconfined concrete stress-strain curve
ϵ_c = concrete strain
ϵ_{cc} = concrete strain at top of section
ϵ_{co} = 0.002 = concrete strain at maximum stress f'_c
ϵ_p = prestressing steel strain
ϵ_{pb} = prestressing steel strain defined in Fig. 4(b)
ϵ_{pc} = prestressing steel strain defined in Fig. 4(b)
ϵ_{pu} = ultimate strain of prestressing steel
ϵ_s = strain in non-prestressed steel
ϵ_{sh} = strain in non-prestressed steel at commencement of strain hardening
ϵ_{su} = ultimate strain of non-prestressed steel
ϵ_y = strain in non-prestressed steel first yield
θ_u = ultimate rotation
θ_y = rotation at first yield
μ = displacement ductility factor = Δ_u/Δ_y
ρ = A_s/bd for non-prestressed steel
ρ' = A'_s/bd for non-prestressed steel
ρ'' = ratio of volume of hoops to volume of confined concrete core
ϕ = curvature, defined as the rotation per unit length of member = ϵ_{cc}/c
ϕ_u = ultimate curvature
ϕ_y = curvature at first yield

* * *